Flexoelectric sensing using a multilayered barium strontium titanate structure

2013 Smart Mater. Struct. 22 115017

(http://iopscience.iop.org/0964-1726/22/11/115017)

Smart Mater. Struct. **22** (2013) 115017 (7pp) doi:10.1088/0964-1726/22/11/115017

Flexoelectric sensing using a multilayered barium strontium titanate structure

S R Kwon[1], W B Huang[1], S J Zhang[2], F G Yuan[1] and X N Jiang[1]

[1] Department of Mechanical and Aerospace Engineering, North Carolina State University, Raleigh, NC 27695, USA
[2] Materials Research Institute, Pennsylvania State University, University Park, PA 16802, USA

E-mail: xjiang5@ncsu.edu

Received 24 April 2013, in final form 23 August 2013
Published 17 October 2013
Online at stacks.iop.org/SMS/22/115017

Abstract
The flexoelectric effect has been recently explored for its promise in electromechanical sensing. However, the relatively low flexoelectric coefficients of ferroelectrics inhibit the potential to develop flexoelectric sensing devices. In this paper, a multilayered structure using flexoelectric barium strontium titanate ($Ba_{0.65}Sr_{0.35}TiO_3$ or BST) ceramic was fabricated in an attempt to enhance the effective flexoelectric coefficients using its inherent scale effect, and hence to improve the flexoelectric sensitivity. The performances of piezoelectric and flexoelectric cantilevers with the same dimensions and under the same conditions were compared. Owing to the flexoelectric scaling effect, under the same force input, the BST flexoelectric structure generated a higher charge output than its piezoelectric P(VDF-TrFE) and PMN-30PT counterparts when its thickness was less than 73.1 μm and 1.43 μm, respectively. Also, amplification of the charge output using the multilayered structure was then experimentally verified. The prototyped structure consisted of three layers of 350 μm-thick BST plates with a parallel electric connection. The charge output was approximately 287% of that obtained using a single-layer structure with the same total thickness of the multilayered structure under the same end deflection input, which suggests high sensitivity sensing can be achieved using multilayer flexoelectric structures.

(Some figures may appear in colour only in the online journal)

1. Introduction

Electromechanical sensors have been developed for automobiles, consumer electronics, biomedical instruments and military systems in order to enhance overall system performance. These sensors need to be small (micro- or nanoscale) and lightweight to reduce the self-loading effect and the cost of manufacturing. Among these different types of sensors, piezoelectric sensors are widely used due to their fast response time, wide frequency bandwidth, ease of use, and low cost [1–4]. However, piezoelectric sensors are being increasingly challenged: as the piezoelectric dimensions are scaled down to the micro/nano domain, the piezoelectricity in thin films and piezonanostructures is significantly degraded [1]. Furthermore, de-poling is another general concern for piezoelectric sensors [5]. Nevertheless, it is important to point out that recent research on the flexoelectric effect has revealed flexoelectric sensing as an alternative technique to piezoelectric sensing [6, 7].

The flexoelectric effect is known to have some unique features in comparison with the piezoelectric effect. First, all insulating solids exhibit flexoelectricity, while piezoelectricity is confined to 20 crystal symmetry groups, thus flexoelectricity offers more selection for electromechanical sensing. In addition, flexoelectric materials do not require poling because the effect is not based on remnant polarization. Therefore flexoelectric materials do not exhibit de-poling or ageing behavior [6]. In contrast, ageing of piezoelectric ceramics occurs rapidly in the first few hours after removal of the poling field [5, 8]. Of particular significance is that, owing to the scaling effect, in contrast to piezoelectric materials, flexoelectric materials are expected to exhibit much higher sensitivity when scaled down to the micro/nano domains [6, 9–11].

Different types of ferroelectric materials, such as lead magnesium niobate (PMN) [12], barium strontium titanate (BST) [13], lead strontium titanate (PST), barium titanate (BT) [14], lead zirconate titanate (PZT) [15] and polymers such as polyvinylidene fluoride (PVDF) [16], polyethylene terephthalate (PET), polyethylene and epoxy [17] have been intensively studied for use in flexoelectric devices. Among these, $Ba_{0.67}Sr_{0.33}TiO_3$ showed the largest flexoelectric coefficient ($\mu_{12} \sim 100\ \mu C\ m^{-1}$) at its Curie temperature of 21 °C. In addition to studies on flexoelectric materials, novel flexoelectric structures with large induced strain gradients have also been studied in order to improve the flexoelectric properties. $Ba_{0.67}Sr_{0.33}TiO_3$ truncated pyramid arrays were designed and fabricated to take advantage of increased strain gradients [18]. Additionally, a flexural mode composite with BST beams was prototyped with an effective piezoelectric coefficient up to 4350 pC N^{-1}, outperforming state of the art lead-based piezoelectric materials [19]. Unimorph-typed micro-cantilevers have also been studied to demonstrate the scaling effect of different types of flexoelectric materials [9, 17].

From previous studies, flexoelectric sensing structures on the millimeter and centimeter scale showed relatively low sensitivity compared to their piezoelectric counterparts [6]. Therefore, output amplification mechanisms are of interest in enhancing the overall performance of flexoelectric devices. Similar amplification mechanisms have been studied in piezoelectric sensing. For example, piezoelectric multilayered structures possess advantages over single-layer piezoelectric structures in many aspects, including a quick response, high voltage/charge sensitivity and high resonant frequency [19–21].

In section 2 we describe a flexoelectric multilayered cantilever structure using BST ceramic that was designed, fabricated and tested. Charge output analysis from piezoelectric and flexoelectric multilayered structures is presented, followed by a comparison between charge outputs from a flexoelectric single-layer and double-layer cantilevers using an analytical model based on the Euler–Bernoulli beam theory. In section 3 we describe experiments performed on a flexoelectric multilayered cantilever. In section 4 we compare the results to those from single-layer cantilever tests and discuss the findings. We close with our conclusions in section 5.

2. Flexoelectric cantilevers

Flexoelectricity refers to the generation of an electric polarization response induced by a mechanical strain gradient (direct flexoelectric effect) or a mechanical strain response induced by an electric field gradient (converse flexoelectric effect). The direct flexoelectric effect can be described by the equation

$$P_l = \mu_{ijkl} \frac{\partial \varepsilon_{ij}}{\partial x_k}, \tag{1}$$

where P_l is the flexoelectric polarization, μ_{ijkl} is the flexoelectric coefficient (a fourth-rank polar tensor with nonzero components $\mu_{11}, \mu_{12}, \mu_{44}$ in a cubic crystal), ε_{ij} is the elastic strain and x_k is the position coordinate.

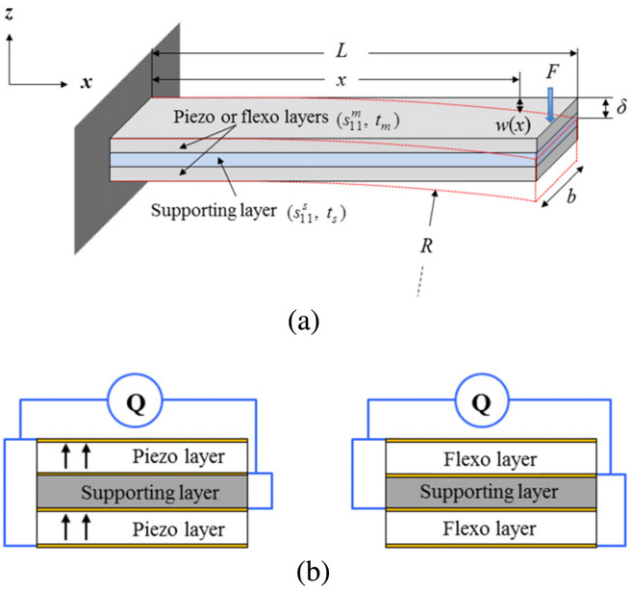

Figure 1. (a) A schematic of a cantilever composed of one supporting layer and two piezoelectric or two flexoelectric layers and (b) side views of the electrical connections in piezoelectric (left) and flexoelectric (right) cantilevers.

2.1. Piezoelectric and flexoelectric cantilever model

The cantilever bimorph structures are usually composed of two active layers (piezoelectric or flexoelectric) and one supporting layer in between, as shown in figure 1(a). In the piezoelectric case, when an external force is exerted at the end of a cantilever, axial normal stress in the piezoelectric layers induces electric polarization. Similarly, in the flexoelectric case, an end force creates a normal strain gradient along the thickness direction of the flexoelectric layers, inducing an electric polarization.

Based on Euler–Bernoulli beam theory, the curvature κ of a cantilever under a bending moment induced by force F at the tip can be given as [22]

$$\kappa = \frac{1}{R} = \frac{12 F s_{11}^{\mathrm{m}} s_{11}^{\mathrm{s}}}{kb}(L - x), \tag{2}$$

where,

$$k = 2s_{11}^{\mathrm{s}}(3t_{\mathrm{s}}^2 t_{\mathrm{m}} + 6t_{\mathrm{s}} t_{\mathrm{m}}^2 + 4t_{\mathrm{m}}^3) + s_{11}^{\mathrm{m}} t_{\mathrm{s}}^3. \tag{3}$$

The superscript or subscript s denotes the supporting layer, m denotes the top and bottom piezo- or flexo-material. x, s_{11}, t, b and R are the axial distance from the clamped end, and the compliance, thickness, width and radius of curvature of the cantilever, respectively.

To amplify the charge output, two layer structures were designed with parallel electrical connections, as shown in figure 1(b). The arrows in the piezoelectric layers denote the poling direction for the piezoelectric cantilever.

The axial normal stress σ_{11} in the piezoelectric cantilever can be expressed as

$$\sigma_{11} = \frac{1}{s_{11}^{\mathrm{m}} R} y_n = \frac{1}{s_{11}^{\mathrm{m}} R}(t_{\mathrm{s}} + t_{\mathrm{m}}) \Big/ 2, \tag{4}$$

where y_n is the distance between the neutral axis and the top surface of the piezoelectric layer, which is half of the total thickness of the cantilever.

The electrical polarization P_{p} from each piezoelectric layer is

$$P_{\mathrm{p}} = d_{31}\sigma_{11}, \tag{5}$$

where d_{31} is the transverse piezoelectric coefficient. The total charge Q_{p} from two piezoelectric layers can be calculated by combining (2), (4) and (5).

$$Q_{\mathrm{p}} = 2\int_0^L P_{\mathrm{p}} b\,\mathrm{d}x = 6d_{31}FL^2(t_{\mathrm{s}} + t_{\mathrm{m}})s_{11}^{\mathrm{s}}/k. \tag{6}$$

For the flexoelectric cantilever, the gradient of the axial normal strain along the thickness direction of the cantilever can be given as

$$\frac{\partial \varepsilon_{11}}{\partial z} = \frac{\partial}{\partial z}\left(\frac{z}{R}\right) = \frac{1}{R}, \tag{7}$$

where ε_{11} is the axial normal strain.

The electric polarization P_{f} from each flexoelectric layer can be written as follows [23]:

$$\begin{aligned} P_{\mathrm{f}} &= \mu_{11}\frac{\partial \varepsilon_{33}}{\partial z} + \mu_{12}\left(\frac{\partial \varepsilon_{11}}{\partial z} + \frac{\partial \varepsilon_{22}}{\partial z}\right) \\ &= [\nu\mu_{11} + (1+\nu)\mu_{12}]\frac{\partial \varepsilon_{33}}{\partial z}. \end{aligned} \tag{8}$$

Here, ν is the Poisson ratio of the flexoelectric ceramic. For pure bending of a beam with $L \gg b \gg t$, the flexoelectric polarization due to the gradient of the axial normal strain ε_{11} in the thickness direction can be simplified as

$$P_{\mathrm{f}} = \mu_{12}^{\mathrm{eff}}\frac{\partial \varepsilon_{11}}{\partial z}, \tag{9}$$

where μ_{12}^{eff} denotes the effective transverse flexoelectric coefficient. For convenience, μ_{12}^{eff} will be abbreviated to μ_{12}. Then, the total charge Q_{f} from two flexoelectric layers can be obtained by combining (2), (7) and (9).

$$Q_{\mathrm{f}} = 2\int_0^L P_{\mathrm{f}} b\,\mathrm{d}x = 12\mu_{12}FL^2 s_{11}^{\mathrm{s}} s_{11}^{\mathrm{m}}/k. \tag{10}$$

The ratio between the charge outputs of the piezoelectric and flexoelectric cantilevers can be derived as

$$\frac{Q_{\mathrm{f}}}{Q_{\mathrm{p}}} = \left|\frac{2\mu_{12}s_{11}^{\mathrm{m}}}{d_{31}(t_{\mathrm{s}} + t_{\mathrm{m}})}\right|, \tag{11}$$

which is inversely proportional to the sum of the thickness of the supporting and piezo/flexoelectric layers when the elastic modulus of piezo/flexoelectric material, size and supporting layer of cantilever are identical, meaning that flexoelectric cantilevers are favorable as micro/nano-sensing structures.

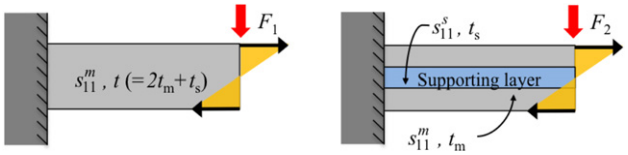

Figure 2. Schematics of a single-layer (left) and multi-layer (right) cantilevers.

2.2. *Multilayered flexoelectric cantilever*

In section 2.1, the analysis showed that the scaling effect can make flexoelectric devices favorable on the micro/nano scale. Another approach to maximizing charge output from flexoelectric sensors involves adopting multilayer structures. Figure 2 shows a single-layer cantilever and a two-layer flexoelectric cantilever structure, where an external force applied at the cantilever tip generates a strain gradient in each layer.

From Bernoulli–Euler beam theory, the strain gradient of the single-layer cantilever is

$$\frac{\partial \varepsilon_{11}}{\partial_z} = \frac{1}{R} = \frac{F_1 s_{11}^{\mathrm{m}}(L-x)}{I}, \tag{12}$$

where L, s_{11}^{m}, I and F_1 are the length, compliance and moment of inertia of a single-layer cantilever and the applied force at the tip, respectively.

The tip deflection of the single-layer cantilever δ_1 can be written as

$$\delta_1 = \frac{F_1 s_{11}^{\mathrm{m}} L^3}{3I}. \tag{13}$$

Then, the total electric charge Q_1 from the single-layer cantilever is given as

$$Q_1 = \int_0^L \mu_{12}\frac{\partial \varepsilon_{11}}{\partial_z} b\,\mathrm{d}x = \mu_{12}\frac{F_1 s_{11}^{\mathrm{m}} bL^2}{2I} = \mu_{12}\frac{3b\delta_1}{2L}. \tag{14}$$

The charge output of the double-layer cantilever can be obtained by (10) and the tip deflection δ_2 when force F_2 is applied at the tip using the expression

$$\delta_2 = \frac{4F_2 L^3 s_{11}^{\mathrm{m}} s_{11}^{\mathrm{s}}}{kb}, \tag{15}$$

where s_{11}^{s} is the compliance of the supporting layer.

By substituting (15) into (10), the charge output from the double-layer cantilever Q_2 can be obtained as

$$Q_2 = \mu_{12}\frac{3b\delta_2}{L}. \tag{16}$$

As shown in (14) and (16), if the input deflection is identical for both cases, the charge output from the double-layer cantilever can be amplified by 200% compared to that from the single-layer cantilever. Similarly, the charge output from a structure with more than two layers will be amplified and is proportional to the number of flexoelectric layers N, as given in (17).

$$Q_n = \mu_{12}\frac{3N\delta_n}{2L}. \tag{17}$$

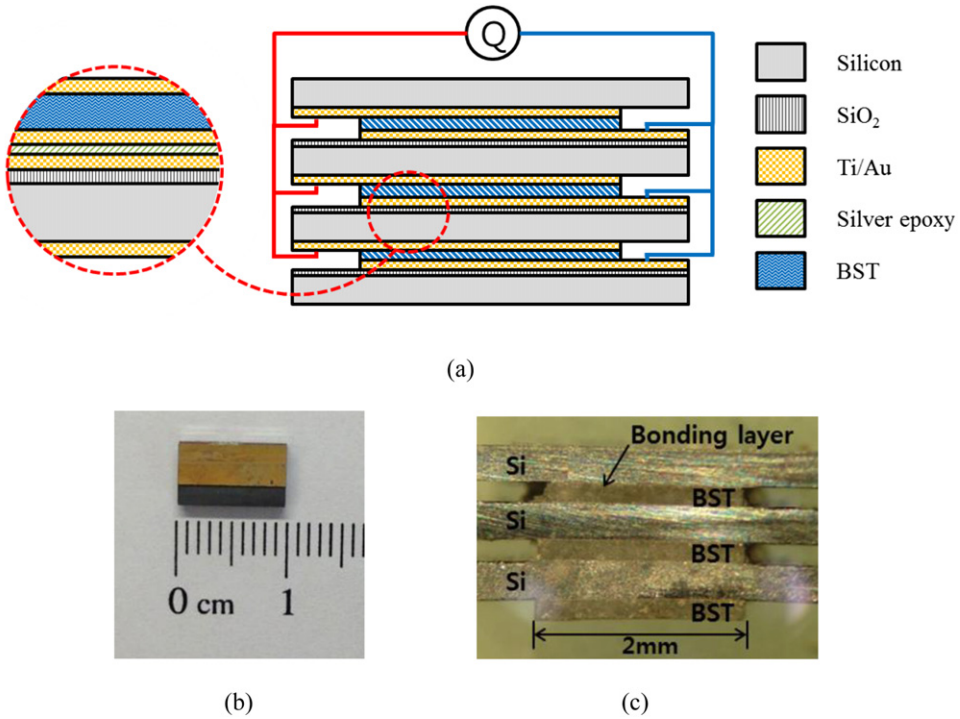

Figure 3. Fabrication of the multilayered structure. (a) A schematic cross-section of the three-layered flexoelectric structure, (b) top view photograph and (c) photograph of a cross-section of the three-layered flexoelectric structure.

3. Experimental methods

3.1. BST material preparation

$Ba_{0.65}Sr_{0.35}TiO_3$ was prepared by conventional solid state processing using raw materials, including $BaCO_3$ (99.9%, Alfa Aesar), $SrCO_3$ (99.9%, Alfa Aesar) and TiO_2 (99.99%, Alfa Aesar). All the materials were weighed for the composition of BST to be Ba:Sr = 65%:35%. The powders were milled in anhydrous ethanol for one day, and then calcined at 1200 °C for 2 h to decompose the carbonate and synthesize the BST powder. The obtained powder was milled and calcined again at the same temperature, then granulated through an 80-mesh sieve. The powder was pressed into pellets with a minimum of 1 inch diameter using cold isotropic pressing at 30 ksi. The pellets were sintered at 1300–1350 °C and cooled down to room temperature at a cooling rate of 3 °C min^{-1} in an oxygen atmosphere. The ceramic had the relative dielectric constant of 8000 at room temperature, and its maximum dielectric constant is about 14 000 at the Curie temperature of 18 °C.

3.2. Fabrication of the multilayered flexoelectric structure

In order to fabricate the multilayered structure, each single layer consisting of BST and silicon layers was fabricated first and three single layers were stacked and bonded consecutively with conductive epoxy. Firstly, a layer of 1 μm of SiO_2 was sputtered on a 350 μm thick silicon wafer in order to prevent shorting of the electrical connection through the BST layer. Here, a 350 μm of silicon layer was chosen because it is easy to handle without breaking. Subsequently, 100 Å of Ti and 1000 Å of Au were sputtered as electrodes on the top and bottom sides of the silicon substrate and on one side of the BST. The sputtered sides of the BST and the silicon substrate were bonded with silver epoxy (Epoxy set, EO-23M). A normal pressure of 1 MPa was applied to produce a bonding layer thickness of about 7–8 μm. This also ensured good adhesion and conductivity between the BST and the silicon substrate. Then, the BST layer was lapped to 25 μm and the top surface of the BST layer was electrode sputtered as mentioned above. Figure 3(a) shows the cross-section of the multilayered structure and the detailed sequence of each layer, while table 1 shows detailed dimensions of the multilayered flexoelectric structure.

Table 1. Dimensions of the three-layered flexoelectric structure.

Thickness of silicon (t_s)	Thickness of BST (t_f)	Total thickness (t_{total})	Length (L)	Width (b)
350 μm	25 μm	1.26 mm	7.5 mm	2 mm

3.3. Experimental setup

To experimentally verify the charge amplification of the flexoelectric multilayered cantilever, the charge output of the fabricated flexoelectric multilayered prototype was measured at room temperature. The experimental setup is shown schematically in figure 4. Firstly, the multilayered flexoelectric structure was clamped rigidly at one end. Then, the piezoelectric actuator was placed at the tip to generate

Table 2. Piezoelectric and flexoelectric coefficients of various materials (see [13, 24–29]).

Lead-based piezoelectric materials	d_{31} (pC N^{-1})	Compliance—s_{11} (10^{-12} m^2 N^{-1})
$PbTiO_3$	−22.8	6.5
PZT (sol–gel)	−82	13.8
PZT (sputtering)	−100	13.3
PMN-30PT	−921	52.0
Lead-free piezoelectric materials	d_{31} (pC N^{-1})	Compliance—s_{11} (10^{-12} m^2 N^{-1})
P(VDF-TrFE)	−18	740.1
PVDF	−28	370.4
$BaTiO_3$ (single crystal)	−33.4	7.4
$K_{0.48}Na_{0.52}NbO_3$ (sputtering)	−45.1	8.2
Flexoelectric material	μ_{12} (μC m^{-1})	Compliance—s_{11} (10^{-12} m^2 N^{-1})
BST	100	6.54

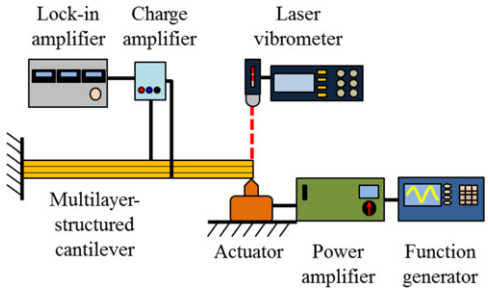

Figure 4. Schematic of the experimental setup for the transverse flexoelectric coefficient measurement.

deflection of the cantilever. The actuator was driven by a power amplifier (Brüel and Kjær, type 2706) and a function generator (Tectronix, Model AFG3101). The deflection of the cantilever at the tip was measured by a laser vibrometer (Polytec, OFV-5000). The generated output signal was amplified by a charge amplifier (Brüel and Kjær, type 2635) and the amplified signal was measured by a lock-in amplifier (Stanford Research system, Model SR830). The generated charge from the single-layer and three-layer cantilevers were recorded as a function of excitation frequency from 1 to 150 Hz. A low frequency was chosen to ensure that the real deflection of the cantilever follows the input of the piezoelectric actuator.

4. Results and discussion

4.1. Modeling results

It is anticipated from (11) that the charge output of the flexoelectric cantilever will exceed that of the piezoelectric cantilever on the micro/nano scales. The ratio of charge output from a BST flexoelectric cantilever to that of a piezoelectric cantilever is shown in figure 5, using the reported material properties given in table 2. When the performance of the BST cantilever is compared with that of a cantilever fabricated from a material with very high piezoelectric coefficients such as PMN-30PT, the thickness of the cantilever must be less than 1.43 μm to yield better performance. When piezoelectric

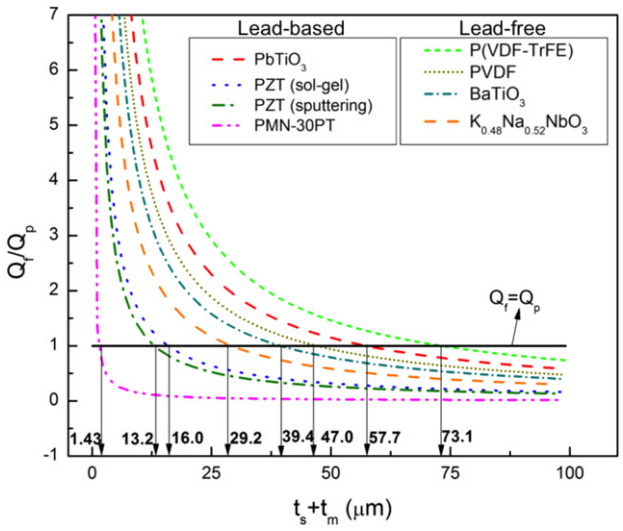

Figure 5. The ratio of charge output from BST flexoelectric cantilevers to that of piezoelectric cantilevers as a function of the total beam thickness.

materials with relatively low piezoelectric coefficients are used, the performance of the flexoelectric cantilever exceeds that of the piezoelectric case on larger scales. For example, the BST flexoelectric device shows much better performance than the piezoelectric device fabricated from P(VDF-TrFE) when the thickness is below 73.1 μm.

4.2. Experimental results

The experiment to measure the charge output from the multilayered cantilever was carried out for sensitivity comparisons with the single-layer cantilever. Charge outputs were measured under different deflections (1–6 μm) and frequencies (1–150 Hz). Experiments were repeated three times under each condition with each data point on the graph representing the average of the three trials. The linear relationship between the deflection at the tip and the charge output can be seen in figure 6. The equivalent transverse flexoelectric coefficient μ_{12}^{e} of the multilayered flexoelectric

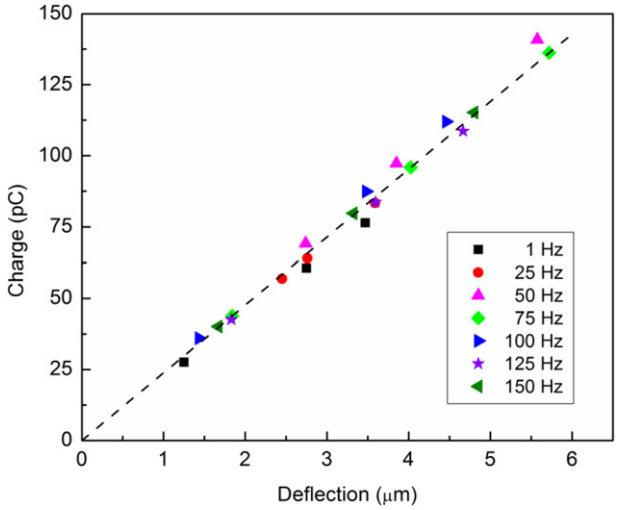

Figure 6. Deflection at the cantilever tip versus charge output from the multilayered flexoelectric cantilever under different force excitation.

structure can be derived from (14) and calculated as

$$\mu_{12}^{\mathrm{e}} = \frac{2QL}{3b^{\delta}}. \tag{18}$$

The average equivalent transverse flexoelectric coefficient μ_{12}^{e} can be calculated from the slope of figure 6 and yields a value of approximately 59.5 μC m^{-1}, which is about three times the magnitude of that of a single-layer flexoelectric cantilever (20 μC m^{-1} [6]). Therefore, when the total dimensions of the flexoelectric structure is the same as the single-layer structure, the sensitivity that is directly related to the equivalent flexoelectric coefficient will be multiplied proportionally by the number of layers. Furthermore, the sensitivity can be further enhanced by choosing intermediate layers with a lower stiffness.

Figure 7 shows the measured equivalent μ_{12} (squares) of the multilayered flexoelectric structure as a function of excitation frequency and the percentage ratio (triangles) of equivalent μ_{12} of a multilayered structure to μ_{12} of a single-layer structure. The dashed lines in the graph denote the average values of the measurements. As seen in figure 7, the transverse flexoelectric coefficient was amplified proportionally to the number of structure layers. The average μ_{12} for the multilayer is slightly less than 300% of μ_{12} for the single-layer flexoelectric cantilever. This could be the result of non-ideal bonding between the BST layers and the supporting silicon layer, which would hinder full strain transfer between each layer. Also, non-perfect clamping could decrease the charge output. The relatively low equivalent μ_{12} (55.1 μC m^{-1}) and the percentage ratio (262.6%) values at 1 Hz were likely caused by imperfect electric insulation of the silicon substrates, which were chosen for fabrication convenience. Charge leakage through the silicon layers could occur because silicon-BST acts as an *RC* circuit and signal degradation cannot be neglected at low frequencies. This can be improved by choosing substrate materials with better insulating performance.

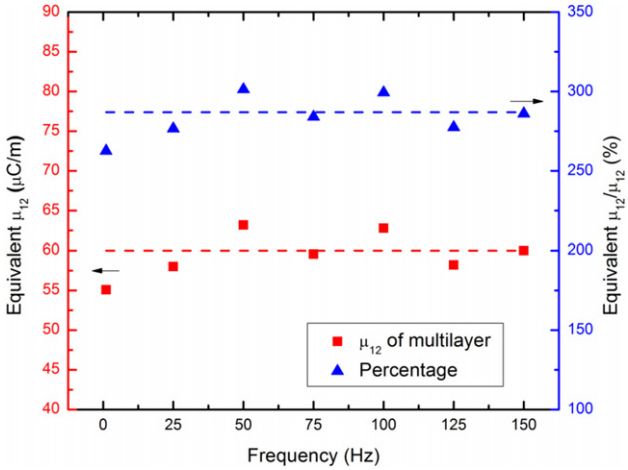

Figure 7. The measured equivalent μ_{12} of the multilayered flexoelectric structure and the ratio of the values of μ_{12} for multilayer to single-layer structures.

5. Conclusions

Flexoelectric sensors are becoming increasingly popular because of their small size, absence of de-poling and ageing problem, and lead-free composition. In this study, a flexoelectric multilayered cantilever was compared analytically to its piezoelectric equivalent and displayed amplified charge output. As the thickness of the cantilever is reduced to the range of several microns, the flexoelectric cantilever is expected to perform with a higher sensitivity than the piezoelectric cantilever. Also, theoretical analysis suggests that the charge output of the multilayer structure is proportional to the number of layers. Finally, a three-layered BST flexoelectric structure for the purpose of amplifying the charge output was successfully fabricated and tested using $Ba_{0.65}Sr_{0.35}TiO_3$ materials. The charge output was measured to be approximately three times that generated by the single-layer structure, confirming the signal amplification mechanism of the multilayered structure.

Acknowledgments

This material is based upon work supported by, or in part by, the US Army Research Laboratory and the US Army Research Office under contract/grant number W911NF-11-1-0516; and in part by National Science Foundation under grant number CMMI-1068345.

References

[1] Yu J-C and Lan C-B 2001 System modeling of microaccelerometer using piezoelectric thin films *Sensors Actuators* A **88** 178–86

[2] Sirohi J and Chopra I 2000 Fundamental understanding of piezoelectric strain sensors *J. Intell. Mater. Syst. Struct.* **11** 246–57

[3] Booij W, Vogl A, Wang D, Tyholdt F, Østbø N, Ræder H and Prume K 2007 A simple and powerful analytical model for MEMS piezoelectric multimorphs *J. Electroceram.* **19** 387–93

[4] Lee C S, Nam H-J, Kim Y-S, Jin W-H, Cho S-M and Bu J-U 2003 Microcantilevers integrated with heaters and piezoelectric detectors for nano data-storage application *Appl. Phys. Lett.* **83** 4839–41

[5] Shepard J F, Chu F, Kanno I and Trolier-McKinstry S 1999 Characterization and aging response of the d31 piezoelectric coefficient of lead zirconate titanate thin films *J. Appl. Phys.* **85** 6711–6

[6] Huang W, Kwon S R, Zhang S, Yuan F-G and Jiang X 2013 A trapezoid shape flexoelectric micro-accelerometer *J. Intell. Mater. Syst. Struct.* at press

[7] Huang W, Yan X, Kwon S R, Zhang S, Yuan F G and Jiang X 2012 Flexoelectric strain gradient detection using $Ba_{0.64}Sr_{0.36}TiO_3$ for sensing *Appl. Phys. Lett.* **101** 252903

[8] Glynne-Jones P, Beeby S and White N 2001 A method to determine the ageing rate of thick-film PZT layers *Meas. Sci. Technol.* **12** 663

[9] Huang W, Kim K, Zhang S, Yuan F-G and Jiang X 2011 Scaling effect of flexoelectric (Ba, Sr)TiO_3 microcantilevers *Phys. Status Solidi RRL* **5** 350–2

[10] Majdoub M, Sharma P and Cagin T 2008 Enhanced size-dependent piezoelectricity and elasticity in nanostructures due to the flexoelectric effect *Phys. Rev.* B **77** 125424

[11] Nguyen T D, Mao S, Yeh Y W, Purohit P K and McAlpine M C 2013 Nanoscale flexoelectricity *Adv. Mater.* **25** 946–74

[12] Ma W and Cross L E 2001 Observation of the flexoelectric effect in relaxor $Pb(Mg_{1/3}Nb_{2/3})O_3$ ceramics *Appl. Phys. Lett.* **78** 2920–1

[13] Ma W and Cross L E 2002 Flexoelectric polarization of barium strontium titanate in the paraelectric state *Appl. Phys. Lett.* **81** 3440–2

[14] Ma W and Cross L E 2006 Flexoelectricity of barium titanate *Appl. Phys. Lett.* **88** 232902

[15] Ma W and Cross L E 2005 Flexoelectric effect in ceramic lead zirconate titanate *Appl. Phys. Lett.* **86** 072905

[16] Baskaran S, He X, Wang Y and Fu J Y 2012 Strain gradient induced electric polarization in α-phase polyvinylidene fluoride films under bending conditions *J. Appl. Phys.* **111** 014109

[17] Chu B and Salem D R 2012 Flexoelectricity in several thermoplastic and thermosetting polymers *Appl. Phys. Lett.* **101** 103905

[18] Zhu W, Fu J Y, Li N and Cross L 2006 Piezoelectric composite based on the enhanced flexoelectric effects *Appl. Phys. Lett.* **89** 192904

[19] Chu B, Zhu W, Li N and Cross L E 2009 Flexure mode flexoelectric piezoelectric composites *J. Appl. Phys.* **106** 104109

[20] Yao K, Zhu W, Uchino E, Zhang Z and Lim L C 1999 Design and fabrication of a high performance multilayer piezoelectric actuator with bending deformation *IEEE Trans. Ultrason. Ferroelectr. Freq. Control* **46** 1020–7

[21] Goldberg R L and Smith S W 1994 Multilayer piezoelectric ceramics for two-dimensional array transducers *IEEE Trans. Ultrason. Ferroelectr. Freq. Control* **41** 761–71

[22] Hibbeler R C and Fan S 2004 *Statics and Mechanics of Materials* (Englewood Cliffs, NJ: Prentice-Hall)

[23] Ma W 2008 A study of flexoelectric coupling associated internal electric field and stress in thin film ferroelectrics *Phys. Status Solidi* b **245** 761–8

[24] Kalinichev A, Bass J, Sun B and Payne D 1997 Elastic properties of tetragonal $PbTiO_3$ single crystals by Brillouin scattering *J. Mater. Res.* **12** 2623–7

[25] Dubois M-A and Muralt P 1999 Measurement of the effective transverse piezoelectric coefficient e31, f of AlN and $Pb(Zr_x, Ti_{1-x})O_3$ thin films *Sensors Actuators* A **77** 106–12

[26] Dargaville T R, Celina M, Elliot J, Chaplya P, Jones G, Mowery D, Assink R, Clough R and Martin J 2005 *Characterization, Performance and Optimization of PVDF As a Piezoelectric Film for Advanced Space Mirror Concepts* (Albuquerque, NM: Sandia National Laboratories)

[27] Wada S, Suzuki S, Noma T, Suzuki T, Osada M, Kakihana M, Park S-E, Cross L and Shrout T 1999 Enhanced piezoelectric property of barium titanate single crystals with engineered domain configurations *Japan. J. Appl. Phys.* **38** 5505

[28] Lee H J, Kim I W, Kim J S, Ahn C W and Park B H 2009 Ferroelectric and piezoelectric properties of NaKNbO thin films prepared by radio frequency magnetron sputtering *Appl. Phys. Lett.* **94** 092902

[29] Cao H, Schmidt H, Zhang R, Cao W and Luo H 2004 Elastic, piezoelectric, and dielectric properties of $0.58Pb(Mg_{1/3}Nb_{2/3})3$–$0.42PbTiO_3$ single crystal *J. Appl. Phys.* **96** 549